



Variability of Ozone Deposition Velocity Over a Mixed Suburban Temperate Forest

Johan Neiryck* and Arne Verstraeten

Research Institute for Nature and Forest, Geraardsbergen, Belgium

OPEN ACCESS

Edited by:

Patrick Stella,
UMR1048 Sciences Pour l'Action et le
Développement Activités, Produits,
Territoires (SADAPT), France

Reviewed by:

Silvano Fares,
Consiglio per la Ricerca in Agricoltura
e l'Analisi dell'Economia Agraria
(CREA), Italy
Mhairi Coyle,
Centre for Ecology & Hydrology,
United Kingdom

*Correspondence:

Johan Neiryck
johan.neiryck@inbo.be

Specialty section:

This article was submitted to
Air Pollution,
a section of the journal
Frontiers in Environmental Science

Received: 25 April 2018

Accepted: 04 July 2018

Published: 06 August 2018

Citation:

Neiryck J and Verstraeten A (2018)
Variability of Ozone Deposition Velocity
Over a Mixed Suburban Temperate
Forest. *Front. Environ. Sci.* 6:82.
doi: 10.3389/fenvs.2018.00082

A 10-year long dataset of half-hourly ozone (O_3) fluxes was used to study the variability in deposition velocity (v_d) over a mixed temperate suburban forest. Average (median) v_d amounted to 0.70 (0.46) $cm\ s^{-1}$, with day- and night-time average (median) of 0.98 (0.73) $cm\ s^{-1}$ and 0.46 (0.30) $cm\ s^{-1}$, respectively. It was found that the precipitation form had a marked impact on v_d and the deposition efficiency (v_d/v_{dmax}), with highest values measured when the canopy was dew-wetted or covered with snow. The analysis further evidenced that traffic volume led to increased deposition due to the presence of chemical reactions between O_3 and nitric oxide (NO) above the canopy surface. During the working week, daytime values of v_d , v_d/v_{dmax} and the O_3 fluxes (F) were found to be significantly higher than the weekend values, especially during the winter half-year. In a next step, half hourly deposition data were aggregated into day- and night-time monthly values, for a correlative study with measured environmental variables. Monthly average night-time/daytime v_d and v_d/v_{dmax} were positively correlated with the relative humidity at the canopy surface ($RH(z_0')$) and negatively correlated with the water levels below the ground surface. During the daytime, monthly v_d and v_d/v_{dmax} were additionally increased during the working-week when traffic volume was high. There existed, however, substantially different weather conditions, in which unaccounted covariates with a totally different meteorological signature controlled the v_d and F . It was speculated that, among other, biogenic volatile compounds (BVOCs) could have contributed to O_3 quenching in some (spring) months with severe drought stress.

Keywords: canopy wetness, deposition velocity, ozone, traffic volume, precipitation form, biogenic volatile organic compounds, flux divergence, nitrogen oxides

INTRODUCTION

Tropospheric ozone (O_3) is a major secondary air pollutant, whose formation occurs when its precursor gases, nitrogen oxides (NO_x) and volatile organic compounds (VOCs) react in the atmosphere in the presence of sunlight (Ashmore, 2005). Tropospheric O_3 is also considered as the third most important contributor to positive greenhouse radiative forcing (IPCC, 2007). Exposure of tropospheric O_3 has been shown to have a direct adverse impact on human health (WHO, 2008) and to be harmful for crop production and forest vitality in many regions of the Northern Hemisphere (Fowler et al., 2009).

Dry deposition by terrestrial landforms is an important removal process of O₃, but dry deposition rates strongly vary among land cover classes (Hardacre et al., 2015). Due to higher turbulence intensity above forest canopies, pollutants can be more readily trapped compared to smooth vegetation (Fowler et al., 1999). There is a paucity of long-term measurements of O₃ deposition over forest vegetation (Mikkelsen et al., 2004; Fares et al., 2010; Rannik et al., 2012) but long-term series are important to study the O₃ dry deposition processes in different climatic and environmental conditions. In addition, new findings regarding O₃ dry deposition schemes must be incorporated in climate models, to assess effects of future climate scenarios on O₃ removal and to predict future vegetative exposure to O₃ under climate change and projected precursor emission reductions (Klingberg et al., 2014; Mills et al., 2016; Zhang et al., 2016; Franz et al., 2017; Sicard et al., 2017). Ozone induced damage may disrupt the hydrological cycle and key biogeochemical cycles, including those of carbon and nitrogen (Schreuder et al., 2001; Paoletti and Grulke, 2010; de Vries et al., 2014; Hoshika et al., 2015; Franz et al., 2017). Overall adverse effects of O₃ exposure might threaten the global terrestrial biodiversity (Fuhrer et al., 2016).

Non-stomatal dry deposition is increasingly been recognized to be crucial for removal of O₃ from the atmosphere (Altimir et al., 2006; Fares et al., 2010; Clifton et al., 2017). There exist, however, multiple pathways of non-stomatal deposition (Cape et al., 2009; Fowler et al., 2009) and this knowledge is required for inclusion in current model parameterizations. A previous analysis of O₃ dry deposition at our site confirmed the importance of non-stomatal deposition (Neiryck et al., 2012). It was found that canopy wetness enhanced the deposition on external surfaces. It was evident, however, that also other

unaccounted environmental variables contributed to the large variability in dry deposition velocity and the way environmental variables interacted was still a matter of conjecture.

In this study, we analyzed a long-term dataset of O₃ fluxes over a suburban temperate mixed forest, acquired from profile measurements. The study aimed especially to elucidate the high variability in dry deposition rates. Attention was paid to the impact of canopy wetness and the traffic volume on the O₃ deposition velocity across the seasons and years. A correlative data-analysis on monthly basis was performed to explore new site-specific relations between the O₃ deposition and measured environmental variables.

MATERIALS AND METHODS

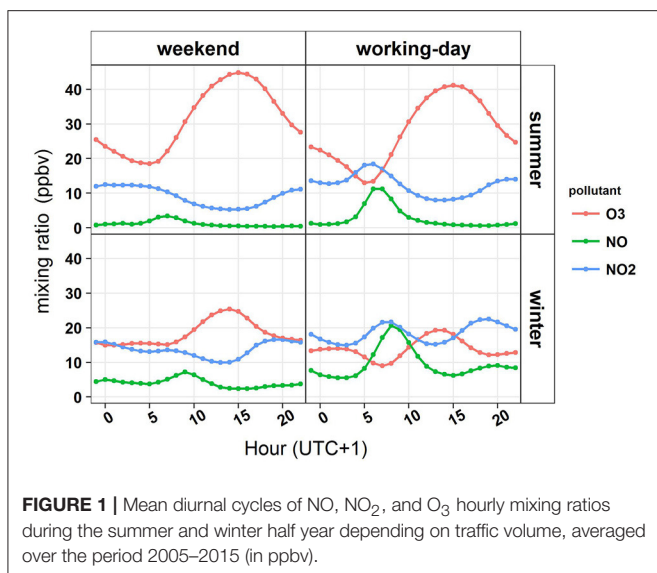
Site Characteristics

The study was conducted in a mixed coniferous/deciduous forest (51°18' N, 4°31' E) near the town of Antwerp, located 10 km to the W from the study site. The forest has a cover of about 300 ha and is nearly uniform in height. It is bordered to the North and West by a residential area within a radius of ca. 500 m (Neiryck et al., 2007). To the South and East, the forested fetch extends over 2 km, before the landscape turns into an agricultural area. The landscape is flat, with a gentle (0.3%) slope at a mean elevation of 16 m. The climate is temperate maritime with a mean annual temperature of 10.8 ± 0.8°C recorded over the period 1996–2015. Annual precipitation averaged 833 ± 112 mm. South-westerly winds are prevailing (>30%).

A 40m high welded scaffold tower is situated in a 2 ha Scots pine (*Pinus sylvestris* L.) stand, planted on former heathland in 1929. Other Scots pine stands can be found in the close vicinity of the measurement tower. More distant from the

TABLE 1 | Percentile distribution of half-hourly deposition velocities (v_d) during the period April 2005 till December 2015 (in cm s⁻¹).

	Winter			Summer		
	Working week	Weekend	All	Working week	Weekend	All
DAYTIME						
10th	-0.03	-0.06	-0.04	10th	0.02	0.04
25th	0.36	0.26	0.32	25th	0.31	0.29
Median	0.91	0.62	0.80	median	0.75	0.62
75th	1.78	1.14	1.58	75th	1.40	1.08
90th	2.99	1.97	2.73	90th	2.35	1.72
Mean	1.22	0.82	1.10	mean	1.00	0.77
<i>n</i>	12,303	5,514	17,817	<i>n</i>	28,205	11,652
NIGHTTIME						
10th	-0.21	-0.14	-0.18	10th	0.09	0.02
25th	0.09	0.09	0.09	25th	0.10	0.10
Median	0.35	0.31	0.34	median	0.27	0.24
75th	0.81	0.65	0.75	75th	0.58	0.49
90th	1.54	1.11	1.40	90th	1.09	0.89
Mean	0.53	0.41	0.49	mean	0.43	0.38
<i>n</i>	27,070	12,357	39,427	<i>n</i>	19,892	8,104



tower (>300 m), forest patches consist of deciduous [mainly pedunculate oak (*Quercus robur* L.) planted in 1936] as well as coniferous species (mainly Scots pine). The tower is located next to a Level II monitoring plot of the pan-European UNECE ICP Forests network and also featured in the CARBOEUROPE and NITROEUROPE research networks. The stand has an open canopy and a mean height of 21 m. Height growth is negligible (± 1 m over 2 decades). The soils supporting the pine trees are Aeolian Coversand layers (Dryas III) with a high sand content >95% (Arenosol). These sandy layers are overlying a substratum of Clay of the Campine (Early Pleistocene Tiglian stage, >40 % clay content), which depth varies between 0.6 and 2 m. A perched water table is present at a variable depth ranging between 0.5 and 3.0 m.

The forest is exposed to different emission sources (Neiryck et al., 2005, 2007). Westerly winds bring sulfur dioxide (SO₂), anthropogenic VOCs and soot bearing air masses, coming either from the petrochemical industry, power plants or other industrial companies situated at the port of Antwerp (15 km to the W). Road traffic and (petro)chemical companies at Antwerp port are also contributing to the high NO_x load at the site. Closer to the site, vehicle exhaust emissions from traffic in the adjacent residential areas and the southerly situated E19 highway (2 km) are the main NO_x emitters. North-easterly winds transport ammonia(NH₃)-bearing air masses, originating from agricultural activities, over the forest. The forest area is also considered to be a source of biogenic VOCs as emitter of monoterpenes from pine trees and isoprenes from oak trees.

Meteorological and O₃ Measurements

Measurements of atmospheric chemistry and meteorology have been conducted at the tower since mid-1995. Air temperature and humidity (HMP 230 dew point transmitter and PT100, Vaisala, Finland) have been measured in aspirated radiation shields at a height of 2, 24, and 40 m. Wind speed has been measured using cup anemometers (LISA cup anemometer,

Siggelkow GMBH, Germany) at 24, 32, and 40 m. At the top of the tower, ingoing and outgoing shortwave and long wave radiation measurements are made by a radiometer (CNR1, pyranometer/pyrgeometer, Kipp and Zonen, the Netherlands). Rainfall is registered by a tipping bucket rain gauge (NINA precipitation pulse transmitter, Siggelkow GMBH, Germany). The leaf wetness is judged by a combination of uncoated leaf wetness grid sensors (Model 237F, Campbell Scientific, Logan, UK) and dielectric Leaf Wetness Sensor (LWS, Decagon devices, USA), which are mounted on a 3-m long boom at the 18 m platform and directed into the canopy. Soil temperature was measured at 2 and 9 cm below soil surface with temperature probes (Didcot DPS-404, UK). Ground water table depth was measured using a PDCR11830 Pressure Transducer (Campbell Scientific, UK).

A fast response infrared gas analyzer (model LI-6262, LI-COR Inc., Lincoln, NE, USA) and a three-dimensional sonic anemometer (model SOLENT, 1012R2, Gill Instruments, Lymington, UK) were installed and operational within the scope of FLUXNET network (<http://fluxnet.fluxdata.org/>). For a detailed description of the Eddy Covariance set-up see Carrara et al. (2003).

Ambient air is drawn from two inlets above the canopy (24 and 40 m) through 53.5-m Teflon sampling tubes with a flow rate of 60 L min⁻¹. Prior to transport, air is filtered through 0.5 mm teflon filter housings, which are covered with a rain shield and mounted at the end of a 1.5-m long boom. The Teflon tubings (external diameter 9.5 mm) are wrapped with 47 mm-isolated housings and heated to 35°C using an electric heating wire. Each inlet is sampled for 5 min before switching to the next inlet using a PLC controlled valve system. Readings of the first minute from every inlet are discarded as sample tubes need to be flushed. Air samples are led toward a manifold in the air conditioned instrument shelter perched on the concrete base of the scaffolding. From the manifold, air is sampled by the monitor, after passing a 0.5 μm filter placed before the sample inlet, removing the smaller dust and soot particles. Ozone concentrations have been measured using a UV Photometric Analyser (period 2000–2007: model TEI 49C, Thermo Environmental Instruments, USA (detection limit: 1 ppb, precision: 0.5 ppb); later replaced by model TEI 49L, Thermo Environmental Instruments, USA (detection limit: 1 ppb, precision: 0.25 ppb). Gaseous NO_x (NO + NO₂ (nitric oxide and nitrogen dioxide, respectively)) concentrations have been analyzed with a chemiluminescence monitor (CLD700 AL, Ecophysics, Switzerland).

Calculation of Fluxes and Resistances

Fluxes (F) are calculated from the Businger-Dyer flux-profile relationships (Businger et al., 1970; Dyer and Hicks, 1970):

$$F = -K \frac{\partial [O_3]}{\partial z} \quad (1)$$

where F is the flux (deposition is defined as negative flux) obtained by multiplying the O₃ gradient from the 24 and

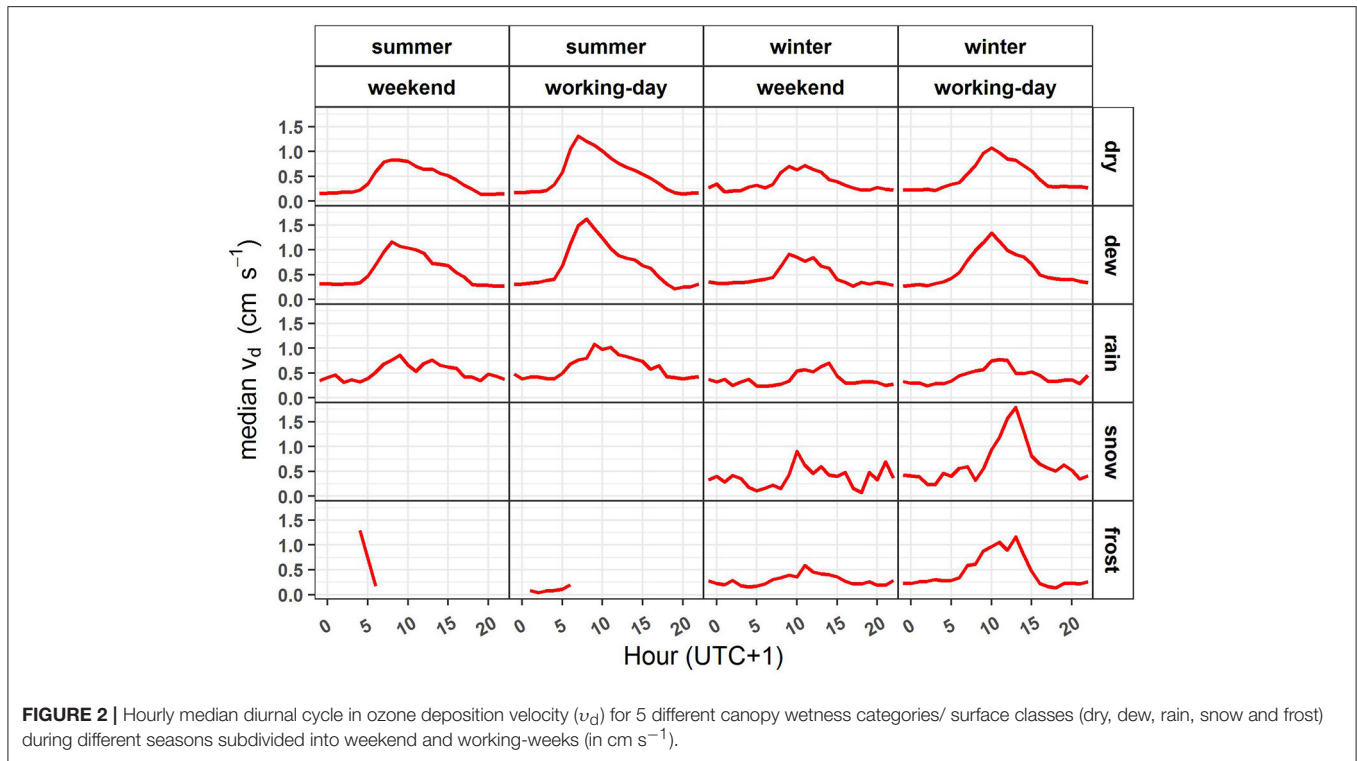


FIGURE 2 | Hourly median diurnal cycle in ozone deposition velocity (v_d) for 5 different canopy wetness categories/ surface classes (dry, dew, rain, snow and frost) during different seasons subdivided into weekend and working-weeks (in cm s^{-1}).

40 m height interval and K , the turbulent diffusivity, which is calculated as:

$$K = \frac{\kappa(z-d)u_*}{\phi_h} \quad (2)$$

In this formula κ (the von Karman constant) is 0.41, z is the geometric mean of the measurement heights (29.7 m), d is the zero plane displacement (17.1 m = 0.8 times the average tree height) and u_* is the friction velocity determined as the square root of the kinematic momentum flux measured by eddy covariance (measuring height 41 m). In order to account for stability effects, the universal flux-profile relationships for heat transfer (ϕ_h) are applied (Dyer and Hicks, 1970). Because the concentration measurements are made in the roughness sublayer, turbulent diffusivities estimated by Equation (2) are corrected by a factor α (= 0.86) to allow for wake turbulence generated above the canopy (Bosveld, 1991):

$$\phi_h = \begin{cases} L \leq 0 \dots \dots \alpha * \left(1 - 16 \frac{(z-d)}{L}\right)^{-\frac{1}{2}} \\ L > 0 \dots \dots \alpha + 5 \frac{(z-d)}{L} \end{cases} \quad (3)$$

where L is the Obukhov length (Monin and Obukhov, 1954) and $(z-d)/L$ is the dimensionless stability parameter.

The deposition velocity (v_d) is obtained from the measured flux (F) by dividing F by difference in the concentration $C_{(z-d)}$ of the measured gradient at $z-d$ (geometric mean of the gradient) and the O_3 concentration inside the leaves C_0 .

$$v_d(z-d) = \frac{-F}{C(z-d) - C_0} = \frac{1}{R_t} = \frac{1}{R_a(z-d) + R_b + R_c} \quad (4)$$

Since O_3 doesn't leave behind any residue in the substomate according to the current knowledge, C_0 is assumed to be zero. The reciprocal of v_d is called the total resistance (R_t) and is defined as the sum of the aerodynamic resistance (R_a), the quasi-laminar boundary layer resistance (R_b) and the canopy resistance (R_c).

The aerodynamic resistance (R_a) is calculated according to Garland (1978):

$$R_a(z-d) = \frac{1}{\kappa u_*} \left[\ln \left[\frac{z-d}{z_0} \right] - \Psi_h \left(\frac{z-d}{L} \right) + \Psi_h \left(\frac{z_0}{L} \right) \right] \quad (5)$$

where z_0 = roughness length (1.5 m), and Ψ_h is the integrated stability correction for heat, estimated following (Beljaars and Holtslag, 1990):

The quasi-laminar sublayer resistance R_b is species-dependent and estimated using semi-empirical relationships presented by Hicks et al. (1987):

$$R_b = \frac{2}{\kappa u_*} \left(\frac{Sc}{Pr} \right)^{2/3} \quad (6)$$

Where Sc and Pr are the Schmidt and Prandtl numbers, respectively.

The efficiency of the canopy surface for pollutant uptake is generally approximated by calculating the canopy resistance (R_c) as inverse of $v_d(z-d)$ minus the atmospheric resistances $R_a(z-d)$ and R_b :

$$R_c = \frac{1}{v_d(z-d)} - R_a(z-d) - R_b \quad (7)$$

TABLE 2 | Mean and median values for half-hourly deposition velocity v_d (cm s^{-1}), deposition efficiency (v_d/v_{dmax} , %) and flux F (ppb m s^{-1}) binned into different classes of canopy wetness, traffic volume, season and time of day.

Wetness	Daytime				Nighttime			
	Working-day		Weekend		Working-day		Weekend	
	Mean	Median	Mean	Median	Mean	Median	Mean	Median
v_d (cm s^{-1})								
Winter								
Dry	1.06	0.82	0.69	0.54	0.43	0.30	0.35	0.27
Dew	1.57	1.24	1.07	0.85	0.63	0.41	0.47	0.36
Rain	0.92	0.72	0.64	0.58	0.51	0.37	0.42	0.32
Snow	1.48	1.17	1.43	0.60	0.65	0.47	0.39	0.26
Frost	1.28	0.93	0.67	0.44	0.47	0.31	0.34	0.24
All	1.22	0.91	0.82	0.62	0.53	0.35	0.41	0.31
Summer								
Dry	0.89	0.68	0.68	0.57	0.28	0.19	0.23	0.17
Dew	1.36	1.03	1.07	0.83	0.53	0.36	0.46	0.32
Rain	1.04	0.81	0.80	0.66	0.64	0.45	0.56	0.41
All	1.00	0.75	0.77	0.62	0.43	0.27	0.38	0.24
v_d/v_{dmax} (%)								
Winter								
Dry	20%	13%	14%	9%	12%	6%	10%	6%
Dew	39%	27%	28%	18%	19%	10%	18%	10%
Rain	20%	12%	17%	12%	12%	7%	10%	7%
Snow	42%	33%	42%	22%	21%	11%	13%	8%
Frost	34%	23%	17%	9%	15%	9%	11%	7%
All	27%	16%	19%	11%	15%	8%	13%	8%
Summer								
Dry	17%	11%	13%	10%	12%	7%	11%	7%
Dew	36%	23%	30%	19%	26%	16%	26%	16%
Rain	24%	17%	19%	14%	21%	13%	20%	14%
All	22%	13%	17%	11%	19%	11%	18%	10%
F (ppb m s^{-1})								
Winter								
Dry	-0.191	-0.161	-0.159	-0.135	-0.059	-0.047	-0.064	-0.049
Dew	-0.145	-0.125	-0.149	-0.124	-0.060	-0.044	-0.060	-0.047
Rain	-0.131	-0.112	-0.117	-0.116	-0.069	-0.057	-0.070	-0.059
Snow	-0.127	-0.106	-0.133	-0.115	-0.056	-0.044	-0.046	-0.037
Frost	-0.117	-0.098	-0.096	-0.086	-0.042	-0.030	-0.048	-0.027
All	-0.169	-0.137	-0.150	-0.126	-0.059	-0.045	-0.061	-0.047
Summer								
Dry	-0.275	-0.234	-0.253	-0.223	-0.071	-0.049	-0.068	-0.047
Dew	-0.223	-0.183	-0.232	-0.189	-0.081	-0.054	-0.084	-0.057
Rain	-0.200	-0.170	-0.191	-0.159	-0.123	-0.086	-0.117	-0.085
All	-0.259	-0.217	-0.244	-0.211	-0.082	-0.055	-0.080	-0.055

The application of this equation fails when emission fluxes are measured. Instead of using the R_c , the deposition efficiency was used as metric for the canopy sink strength. The latter is defined as the ratio of the v_d to the maximum deposition allowed by turbulence, v_{dmax} , which was calculated as follows:

$$v_{dmax} = \frac{1}{R_a(z - d) + R_b} \quad (8)$$

The “surface” temperature ($T(z_0')$) and water vapor pressure ($e(z_0')$) were computed from measured micrometeorological fluxes of both sensible (H , W m^{-2}) and latent heat (λE , $\text{J m}^{-2} \text{s}^{-1}$), following Monteith and Unsworth (1990):

$$T(z_0') = T(z - d) + \frac{H}{\rho C_p} (R_a(z - d) + R_b) \quad (9)$$

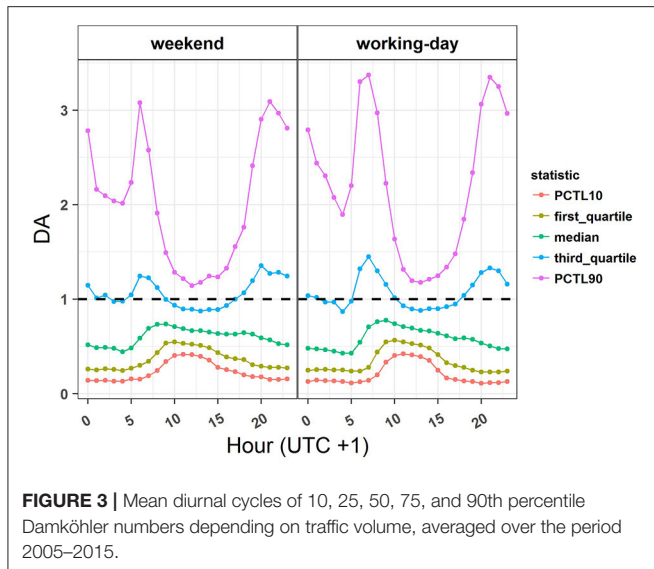


FIGURE 3 | Mean diurnal cycles of 10, 25, 50, 75, and 90th percentile Damköhler numbers depending on traffic volume, averaged over the period 2005–2015.

And

$$e(z_0') = e(z-d) + \frac{pE}{\rho E} (R_a(z-d) + R_b) \quad (10)$$

where T is ambient temperature ($^{\circ}\text{C}$), e is water vapor pressure (kPa), p is atmospheric pressure (kPa), E is the water vapor flux (kPa m s^{-1}), C_p is specific heat of moist air ($\text{kJ kg}^{-1} \text{ }^{\circ}\text{C}^{-1}$), ε is the ratio of the molecular weight of water to the mean molecular weight of dry air (18/29) and ρ is the air density (g m^{-3}). The surface relative humidity ($RH(z_0')$) is given by:

$$RH(z_0') = \frac{e(z_0')}{(e_{\text{sat}} T(z_0'))} \quad (11)$$

where $e_{\text{sat}}(T(z_0'))$ is the saturation water vapor pressure at $T(z_0')$.

Data Handling, Analysis and Statistics

Prior to data analysis, data were checked to allow a proper use of flux-gradient theory. In order to reduce the relative errors in the concentration gradients, concentrations below 1 ppb were excluded. Friction velocities below 0.1 m s^{-1} were rejected as flux-profile relationships might probably be invalid. To avoid non-stationarity problems, data were excluded for which half-hour changes in concentrations led to changes in v_d exceeding 0.01 m s^{-1} ($|((z-d)/c^*(dc/dt)| > 0.01 \text{ m s}^{-1})$). Outliers in the data were removed, rejecting any v_d exceeding $v_{d\text{max}}$, by more than a factor of two.

The flux triad $\text{NO-NO}_2\text{-O}_3$ is subjected to (photo-)chemical reactions, which might lead to chemical sources and sinks of these gases within the layer represented by the measurements. In order to judge possible vertical flux divergence between the surface and the measuring height due to the presence of chemical reactions, the Damköhler number (DA) (Damköhler, 1940) is applied. DA is calculated as the ratio of the transport time (τ_{trans}) and the characteristic chemical timescale (τ_{chem}):

$$DA = \frac{\tau_{\text{trans}}}{\tau_{\text{chem}}} \quad (12)$$

The formula for transport time (τ_{trans}) above the canopy was adopted from Garland (1978)

$$\tau_{\text{trans}} = R_a(z-d) \cdot (z-d-z_0) \quad (13)$$

The chemical reaction time for the $\text{NO-O}_3\text{-NO}_2$ triad (τ_{chem}) was estimated according Lenschow (1982):

$$\tau_{\text{chem}} = \frac{2}{[j_{\text{NO}_2} + k_r^2 \cdot (\text{O}_3 - \text{NO})^2 + 2 \cdot j_{\text{NO}_2} \cdot k_r \cdot (\text{O}_3 + \text{NO} + 2 \cdot \text{NO}_2)]^{0.5}} \quad (14)$$

where k_r ($=44.4 \exp(-1370/(T + 273.15))$) in $\text{ppm}^{-1} \text{ s}^{-1}$ is the reaction rate of the titration reaction of O_3 with NO and j_{NO_2} is the photolysis frequency.

A DA number above unity implies that chemical reactions occur significantly faster than the turbulent transport (flux divergence), whereas DA smaller than 0.1 indicates that the chemistry is too slow to affect the gradients. The range in between is considered as a critical range, where an impact of chemistry cannot be excluded (Stella et al., 2012). In addition, τ_{deplO_3} , the characteristic chemical depletion time for O_3 was calculated according to Vilà-Guerau de Arellano and Duynkerke (1992) as:

$$\tau_{\text{deplO}_3} = \frac{1}{k_r [\text{NO}]} \quad (15)$$

Data on fluxes and deposition velocities were binned according to time of the day, traffic volume (working week with high NO_x levels vs. weekend) and canopy wetness. The differentiation between day and night was based on solar radiation using a threshold of 50 W m^{-2} . Winter half-year (dormant season) was defined as the period running from October till March. Data were further subdivided into five broad macroscopic wetness classes representing differences in the nature of precipitation:

- Dry canopy: reading leaf wetness sensor = 0; absence of visible (macroscopic) wetness but thin moisture films or deliquescent particles might still occur;
- Dew-wetted canopy: reading leaf wetness sensor > 0 but no important preceding rainfall;
- Rain-wetted canopy: contained following cases: rainfall recorded by rain gauge reading leaf wetness sensor > 0 due to precipitation in preceding 4 h (> 1 mm)
- Frost: in case temperatures dropped below 0°C
- Snow: freezing conditions accompanied by a significant change in albedo index (from 9% till 20% and higher), indicating the presence of a (shallow) snow cover on the canopy or the forest soil.

Statistical analyses were performed with R 3.2.2 (R Development Core Team, 2015). Data were aggregated on monthly basis for daytime and night-time conditions. An analysis of covariance (ANCOVA) was conducted with one nominal variable (traffic volume) and continuous predictor variables (maximum amount of allowed turbulence ($v_{d\text{max}}$), vapor pressure deficit (VPD), relative humidity and temperature at the canopy surface ($RH(z_0')$ and $T(z_0')$, resp.), level of water below ground surface

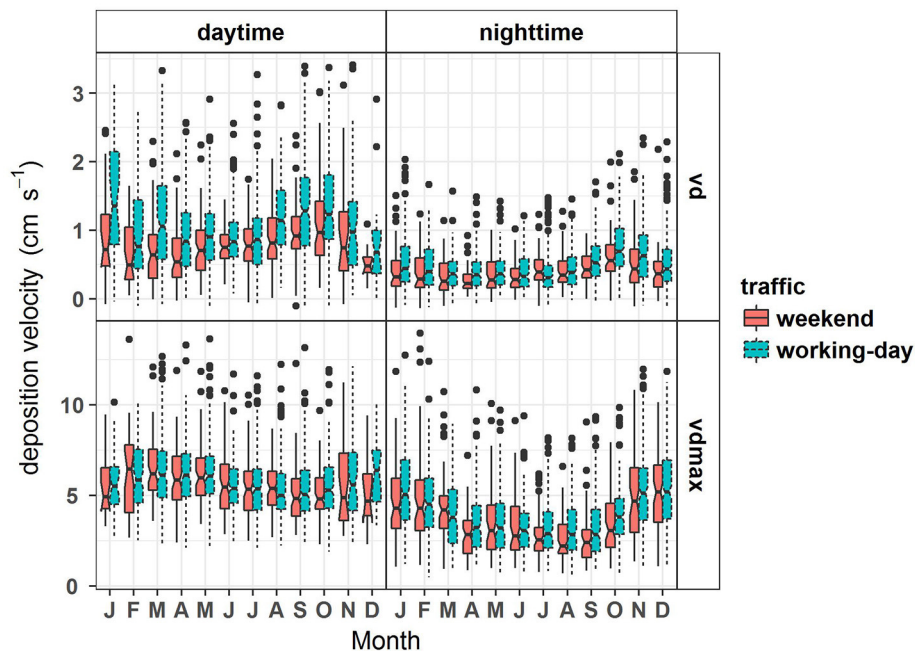


FIGURE 4 | Annual pattern of daily deposition velocity (v_d) and daily maximum deposition velocity allowed by turbulence (v_{dmax}) for weekends and working-days during daytime/nighttime from April 2005 till December 2015 (in cm s^{-1}). The box shows the interquartile range (IQR) of the daily v_d or v_{dmax} for a given month. The whiskers add 1.5 times the IQR to the 75 percentile and subtract 1.5 times the IQR from the 25 percentile. The “Notch” displays the confidence interval around the median which is normally based on the median $\pm 1.57 \times \text{IQR}/\sqrt{n}$. If two boxes’ notches do not overlap there is “strong evidence” (95% confidence) their medians differ.

(gwt), soil temperature (T_s), solar radiation (Sun), precipitation amount and interactions between them. Prior to the ANCOVA, collinearity was detected using pairwise scatterplots and variance inflation factors (VIF). Variables with VIF values above 3 were rejected for further analysis. The final model was obtained using a backward elimination procedure starting from a full (linear or GAM) model. Differences among wetness categories or traffic volume were verified using a Kruskal–Wallis test.

RESULTS

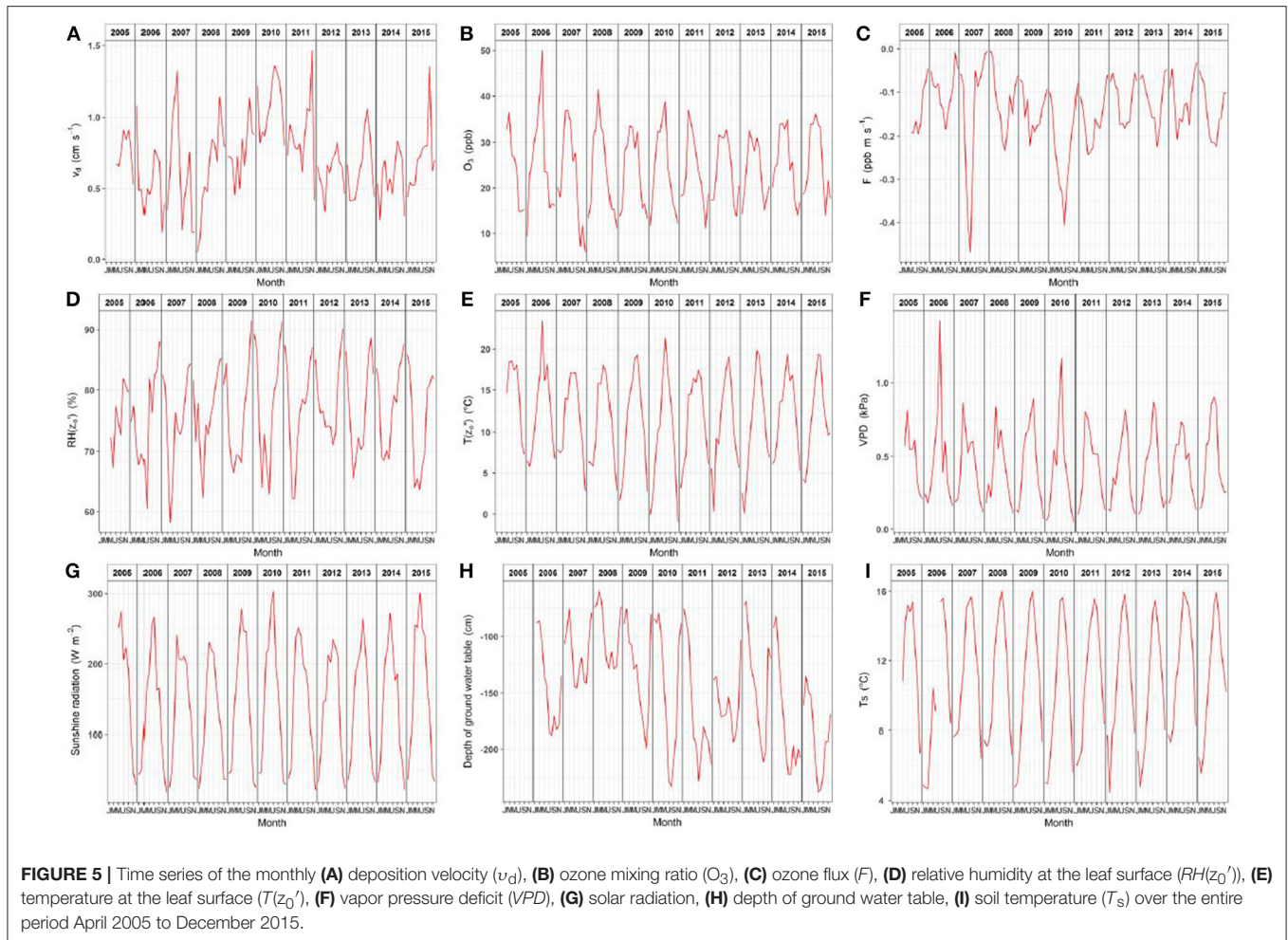
Impact of Traffic Volume and Canopy Wetness on Half Hourly Deposition Velocity

A dataset of 125,097 half-hourly fluxes was retained for statistical analysis for the period April 2005–December 2015, implying a data coverage of 67%. The long-term average (median) O_3 flux (F) from the selected dataset was -0.142 (-0.088) ppb m s^{-1} , corresponding to an average (median) O_3 concentration of 24.8 (23.4) ppb and v_d of 0.70 (0.46) cm s^{-1} . Eleven per cent of the F were upward and they occurred especially during the winter nights (Table 1).

Average v_d during the summer half-year was 0.93 and 0.41 cm s^{-1} for daytime and night-time, respectively. During the winter half-year, measured average v_d were found to be slightly higher (1.1 and 0.49 cm s^{-1} , for daytime and night-time respectively). During the daytime, high traffic volume significantly ($p < 0.0001$) increased v_d , with larger values especially being measured during

the winter working-days (1.22 cm s^{-1}), when a larger chemical sink of NO was present (Figure 1). The lower daytime winter v_d s during the weekend (0.82 cm s^{-1}) were partly outweighed by higher weekend O_3 concentrations (3–4 ppbv) (Figure 1). Daytime differences in v_d due to traffic volume were less marked during the summer half-year but still significant (1.0 vs. 0.77 cm s^{-1} for working-days and weekends, respectively, $p < 0.0001$). Impact of traffic volume on night-time v_d was smaller and only significant during the winter half-year ($p < 0.0001$).

The impact of traffic volume became also evident when data were further binned into five canopy wetness categories, for which a dry (52% of all cases) and dew-wetted canopy (33% of all cases) were the most prominent (Figure 2, Table 2). During the weekend, when the chemical sink was low, largest daytime v_d values ($\pm 1 \text{ cm s}^{-1}$) were observed when the canopy was dew-wetted or when soil/canopy was covered with snow. During the working-week, v_d s substantially rose as a consequence of the enhanced traffic volume in the neighborhood and/or the increased NO_x load originating for Antwerp port (Figures 1, 2). The enhancement was especially evident during the winter working-days (Table 2), with average v_d s for all canopy wetness classes being increased by 50% (compared to 30% during the summer working-days). The shape of the diurnal patterns strongly depended on season and canopy wetness. During the summer half-year, it was found that the daily course of v_d was skewed toward the morning hours for a dry and dew-wetted canopy (Figure 2). There was a steep rise in v_d from

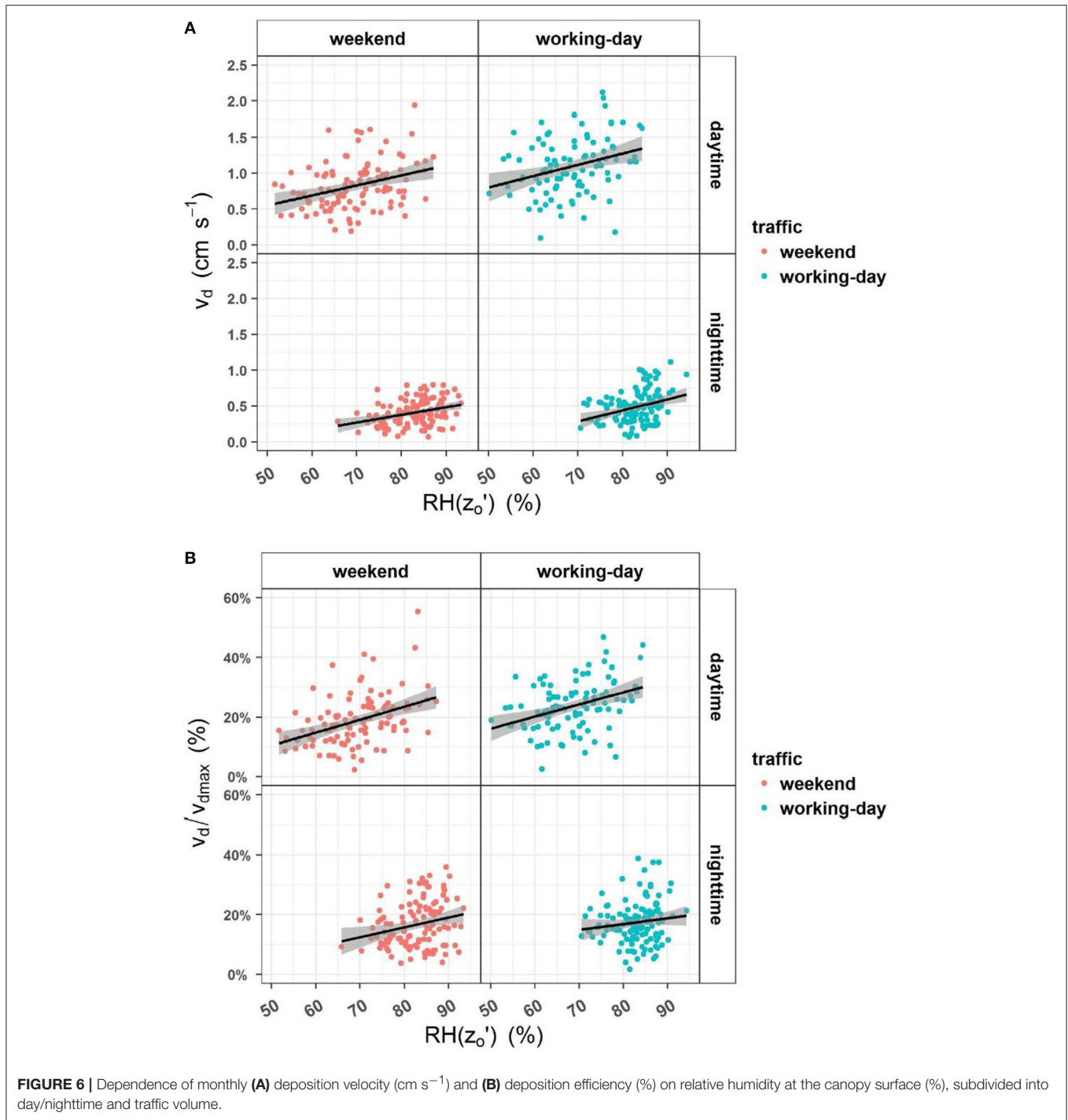


4:00 o'clock onwards with a peak at 8:00, followed by a gentle linear decline toward a nocturnal level, coinciding with stomatal closure. During the winter half-year, the curve of v_d was rather bell-shaped with a broad peak at 10:00 (dry or dew wetted) or at noon (rain, frost, snow), rather following the course of mechanical turbulence.

The findings about v_d were further corroborated by expressing v_d as proportion of the maximum amount available for deposition (v_{dmax}), which might differ among wetness classes or seasons (Table 2). Average deposition efficiency (v_d/v_{dmax}), increased from 19% till 27%, due to increased traffic volume during the winter daytime. The enhancement of v_d/v_{dmax} during the summer daytime hours was less marked but still significant ($p < 0.0001$). The night-time v_d/v_{dmax} was only affected during the winter working-weeks because of more elevated NO values during the evening commuting hours (Figure 1). The v_d/v_{dmax} increased for all canopy wetness categories, except for snow conditions for which available data were scarce (<1%). Due to differences in turbulent regime, differences in v_d/v_{dmax} among dew-wetted, dry or rain-wetted canopy wetness categories were more explicit than when only v_d was considered. During the daytime, v_d/v_{dmax} for a dew-wetted canopy was found to be

almost twice as high compared to a dry or rain wetted canopy. A rain-wetted canopy became a more efficient sink during the summer nights compared to the winter nights.

Average daytime fluxes (F) were 13 and 6% higher during winter and summer working-weeks, respectively (Table 2). Nocturnal F were not affected by traffic volume, as lower v_d s during the weekend were outweighed by concomitant higher O_3 concentrations. The 10-year hourly median DA numbers varied between 0.4 and 0.8, implying that chemical reactions between O_3 and NO between the canopy surface and the measuring height might have occurred, especially during the daytime (Figure 3). The third quartile values and 90 percentile values from the DA numbers exceeded 1, especially during the night-time (due to low turbulence, high τ_{trans}) and the commuting hours, indicating that a flux divergence for the NO-NO₂-O₃ triad was evident above the canopy. The long-term median timescale for O_3 depletion (τ_{deplO_3}) amounted to 3753 s (63 min) and 1665 s (28 min) for weekends and working-days, respectively. This implied that half-hourly gradients were especially affected when traffic volume was high (higher NO concentrations). The lowest long-term median τ_{deplO_3} was calculated for nocturnal winter working-days [956 s (16 min)],



daytime winter working-days [1014 s (17 min)] and daytime summer working-days [2356 s (39 min)]. In these conditions, the highest enhancement of the deposition metrics occurred (Table 2).

With regard to the flux magnitude, dry and dew-wetted canopies trapped most of the O_3 during the daytime. At night, the dry deposition flux was still found to be substantial and be the highest for rain-wetted canopies.

Monthly Variability in v_d

A high monthly variability in daytime v_{dS} was observed throughout the year, with higher v_{dS} measured during the months September, October, November and January (Figure 4). The impact of traffic volume was pronounced during the daytime and especially during the winter half-year. The annual pattern during the night-time was less marked compared to daytime conditions, but also increased daily v_{dS} were measured during

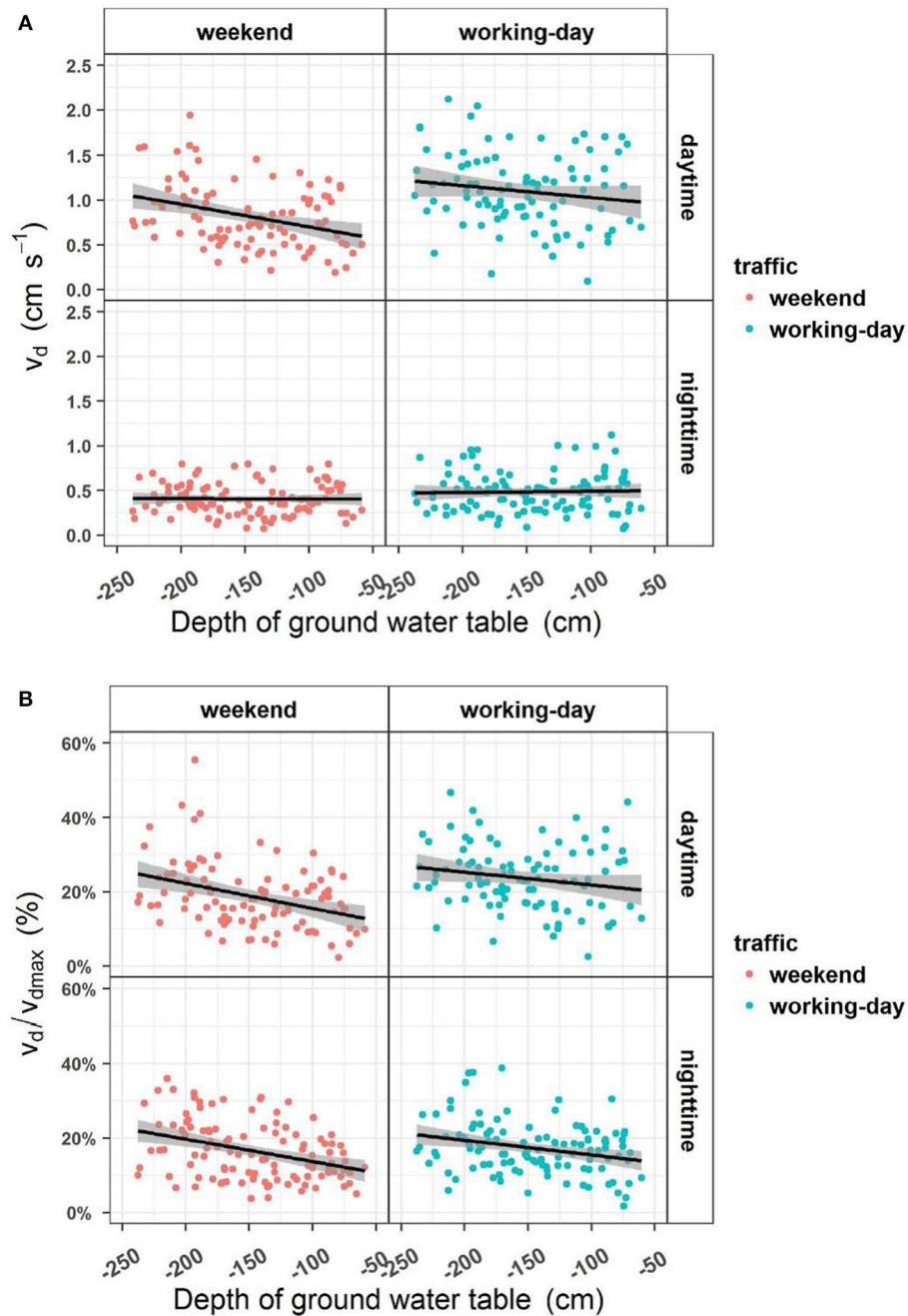


FIGURE 7 | Dependence of monthly (A) deposition velocity (cm s⁻¹) and (B) deposition efficiency (%) on ground water table depth (cm), subdivided into day/nighttime and traffic volume.

the months September, October and November. Impact of traffic volume on monthly variability was less pronounced during the night-time and confined to the winter half-year. The increased v_{ds} toward autumnal months cannot be explained by increased turbulence, since v_{dmax} tended to reach minimum values during these months, especially during the daytime (Figure 4).

The v_d was also subjected to a large interannual variability, with higher v_{ds} reached in 2010 and 2011 (Figure 5A). Measured

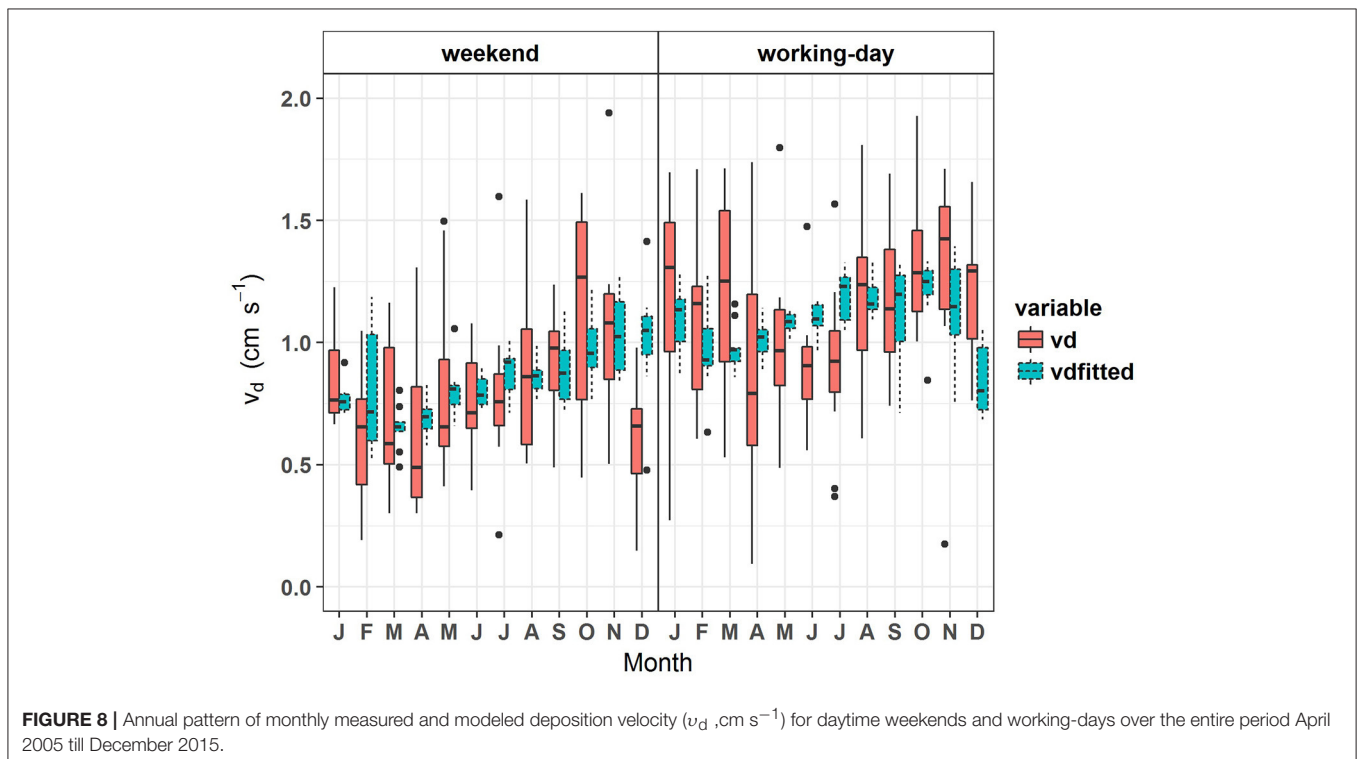
annual mean v_d in the latter years amounted to 1.06 and 0.84 cm s⁻¹, respectively, which is considerably higher than the long-term mean of 0.7 cm s⁻¹. Lowest annual mean v_d was measured during 2006 and 2014 (resp. 0.52 and 0.55 cm s⁻¹).

Results of the analysis of covariance revealed the significant impact of traffic volume, relative humidity and level of ground water table on v_d and v_d/v_{dmax} without interactions implying

TABLE 3 | Results from the analysis of covariance.

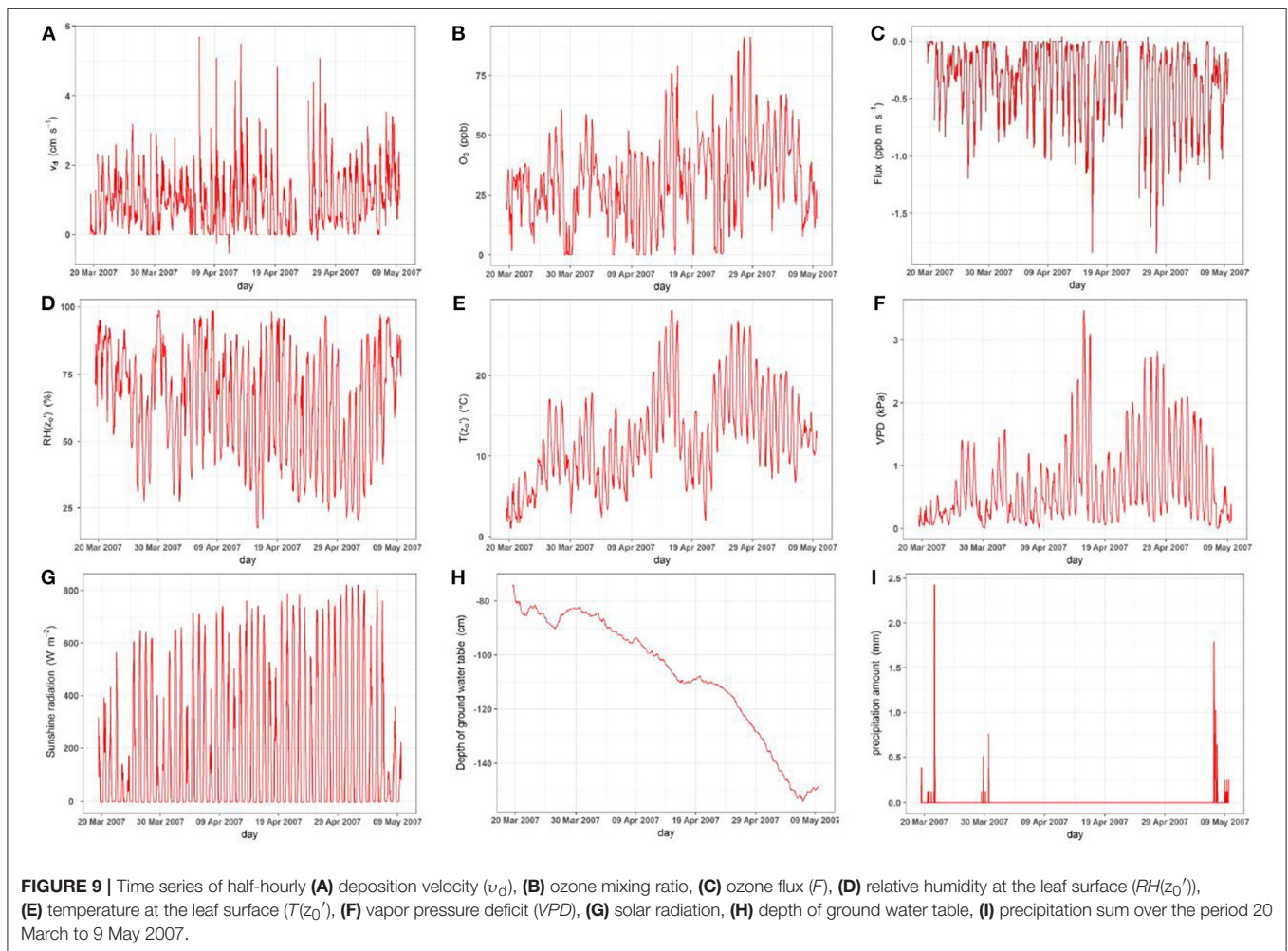
Variable	Daytime			Nighttime		
	Coefficient	Std error	P	Coefficient	Std error	P
v_d (cm s⁻¹)						
Intercept	-0.0373	0.3521	0.9158	-0.6176	0.2012	0.0024
RH	0.0134	0.0032	<0.0001	0.0128	0.0024	<0.0001
Trafficvolume-workingday	0.296	0.0529	<0.0001	0.0805	0.0252	0.0016
gwt	-0.0019	0.0006	0.0016	0.0003	0.0003	0.3497
v_{dmax}	-5.9879	3.3913	0.0791			
R^2	0.27			0.15		
df	188			222		
v_d/v_{dmax} (%)						
Intercept	-0.1854	0.0544	0.0008	-0.0721	0.0742	0.3319
RH	0.0042	0.0007	<0.0001	0.0021	0.0001	0.0233
Trafficvolume-workingday	0.0519	0.012	<0.0001	0.0007	0.0009	0.4403
gwt	-0.0006	0.0001	<0.0001	-0.00004	0.0001	<0.0001
R^2	0.28			0.12		
df	188			222		

Estimated regression coefficients and statistics relating selected average monthly environmental variables [RH (relative humidity), gwt (ground water table) and v_{dmax} (maximum v_d allowed by turbulence)] and one nominal variable (traffic volume: weekend or working-day) to deposition velocity (v_d) and deposition efficiency (v_d/v_{dmax}) during daytime and nighttime conditions.



that effects were probably mainly acting in an additive way (Figures 6A,B, 7A,B, Table 3). Impact of traffic was more explicit during the daytime analysis, where traffic volume increased the v_d by 0.296 cm s⁻¹ ($p < 0.0001$). The analysis further revealed

a positive correlation with $RH(z_0')$ ($p < 0.0001$) and a negative correlation with ground water table depth ($p = 0.0016$) during the daytime. There was also a slight negative relation with v_{dmax} , which was also obvious from Figure 4. With regard to



v_d/v_{dmax} , an enhancement by 5.2% was found during working-days ($p < 0.0001$), along with a positive correlation with $RH(z_0')$ ($p < 0.0001$) and a negative correlation with the depth of the ground water table ($p < 0.0001$). During the night-time, traffic volume slightly enhanced v_d by 0.08 cm s^{-1} ($p = 0.0016$). The ANCOVA revealed a positive contribution from $RH(z_0')$ to v_d/v_{dmax} ($p < 0.0001$) but not from the ground water table depth ($p = 0.35$). When analyzing night-time v_d/v_{dmax} as response variable, no significant impact of traffic volume could be substantiated ($p = 0.44$). There was, however, again a positive correlation with $RH(z_0')$ ($p = 0.02$) and a negative correlation with the ground water table depth $p < 0.0001$.

Although explained variability from the ANCOVA was low (varying between 12 and 28%), deposition on external wet surfaces and especially soil uptake could be useful to understand the annual pattern with increased v_d during the autumnal months, especially during the daytime (Figure 8). The found relationships could, however, not be generalized, especially when data were analyzed on a shorter time-scale. It was clear that in some (spring) months other unaccounted variables (e.g., monoterpene emission) controlled the deposition at the site. In April 2007 e.g., the site was struck by a 40-day lasting drought

period, which led to excessively high F ($< -0.5 \text{ ppb m s}^{-1}$) and high v_d ($> 2 \text{ cm s}^{-1}$), which were rarely encountered during the 10-year monitoring period (Figures 5, 9). The drought stress was accompanied by a rapidly decreasing ground water level, low $RH(z_0')$, high VPD , high $T(z_0')$ and high solar radiation compared to the long-term monthly average. A high correlation between v_d and the solar radiation was found ($p < 0.0001$) (Figure 10). For relative humidity, the negative correlation contrasted with findings from previous monthly analysis. The level of ground water was uncorrelated with v_d . The fluxes were positively correlated with $RH(z_0')$ ($r = 0.7$), VPD ($r = -0.7$), $T(z_0')$ ($r = -0.6$) and solar radiation ($r = -0.8$) (Figure 11).

DISCUSSION

Impact of Traffic Volume

The analysis showed that daytime v_d , v_d/v_{dmax} and F were substantially higher during the working-weeks (Table 2). The presence of large amounts of NO, advected from neighboring vehicle emissions and the more remote port activities in Antwerp led to an increased destruction of O₃ by NO between the canopy surface and the measuring height. Average daytime fluxes during

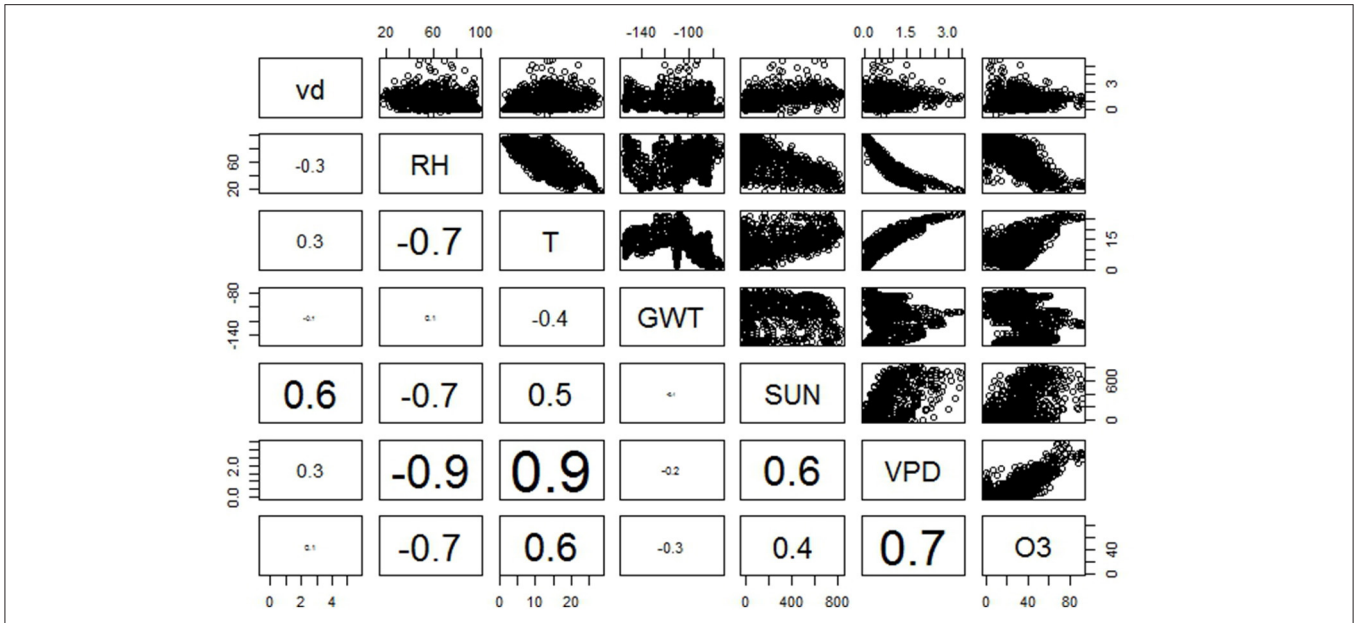


FIGURE 10 | Pairplot of half-hourly deposition velocity ($v_d, \text{cm s}^{-1}$) and covariates measured over the period 20 March to 9 May 2007. The upper panel contains scatterplots while the lower panel depicts the estimated pair-wise Pearson correlations using a font size which is proportional to the absolute value of the estimated correlation coefficient.

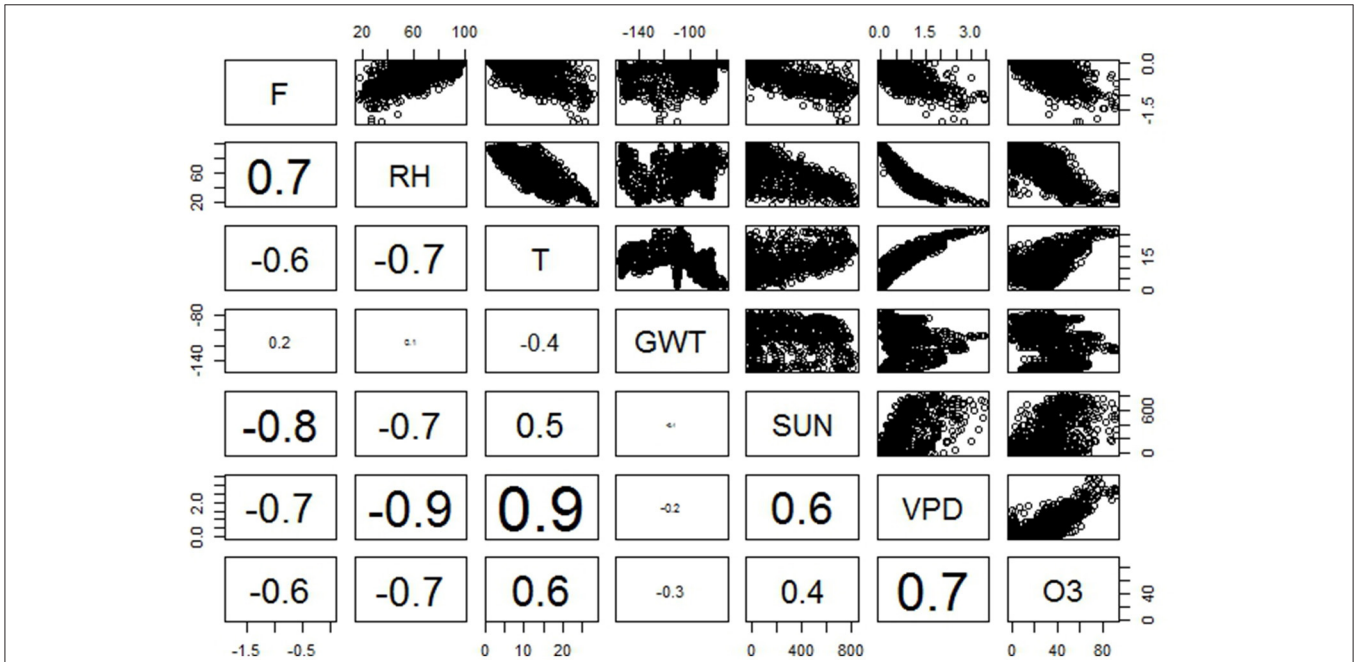


FIGURE 11 | Pairplot of half-hourly ozone flux ($F, \text{ppb m s}^{-1}$) and covariates measured over the period 20 March to 9 May 2007. The upper panel contains scatterplots while the lower panel depicts the estimated pair-wise Pearson correlations using a font size which is proportional to the absolute value of the estimated correlation coefficient.

the working-weeks were 13 and 6% higher during winter and summer, respectively. Median DA numbers varied between 0.4 and 0.8 indicating that photochemical reactions between O_3 , NO , and NO_2 could not be excluded. The lowest long-term

median depletion time for O_3 was recorded for nocturnal winter working-days (16 min), daytime winter working-days (17 min) and daytime summer working-days (39 min). In these conditions, the half-hourly O_3 gradients (and the derived

deposition metrics) were increasingly influenced by chemical reactions with NO. The resulting flux divergence recorded at our site (13 and 6% during winter and summer working-weeks compared to weekend as reference) is within the 0 and 25% deviance range from the surface fluxes for the critical zone of Damköhler number ($0.1 < DA < 1$), as demonstrated by Stella et al. (2012).

The chemical climate during the weekend, characterized by lower NO values, increased ratio of NO₂/NO_x leading to higher presence of O₃, has been amply described by several authors (Fujita et al., 2003; Wolff et al., 2013). Due to a lower chemical sink during the weekends, flux measurements were less affected by flux divergence and hence, they could better represent the intrinsic O₃ deposition to the ecosystem. The average annual daytime and night-time v_d of 0.8 and 0.4 cm s⁻¹, respectively, should therefore preferably be retained as ecosystem v_d for O₃ at our site. The same holds for the dry deposition fluxes, for which the daytime fluxes of -0.150 and -0.244 ppb m s⁻¹ could be considered to be the representative average dry deposition for winter and summer half-year, respectively.

Drivers of Non-stomatal Deposition

Non-stomatal deposition comprises O₃ deposition to the soil surface, woody tree parts, foliage along with gas-phase chemical losses involving reactions between O₃ and BVOCs (biogenic volatile organic compounds) or biogenic NO, which can be either emitted by leaves or soils (Cape et al., 2009). Non-stomatal deposition was considered to be the main deposition pathway at the site (Neiryck et al., 2012). An analysis of covariance showed that increased relative humidity at the leaf surface and lowered ground water tables enhanced both v_d and v_d/v_{dmax} . The nature of the precipitation also controlled the overall uptake of O₃ at the canopy surface during both summer and winter. An intercomparison among canopy wetness classes revealed that v_d and v_d/v_{dmax} was the highest when the canopy was dew-wetted or in case a shallow snow cover was present on the foliage or soil. Wetness effects also impacted the magnitude of the nocturnal O₃ fluxes, which still comprised one third of the daytime O₃ flux. The foliage of this suburban forest is exposed to the corrugating and erosive impact of air pollution, which consists of a mixture of reactive gases (O₃, NH₃, SO₂, and NO_x) and particles (soot, diesel particulate matter, particulate ammonium and nitrate), emitted from different sources (Neiryck et al., 2007, 2011). This results in erosion of the epicuticular waxes of the needles (Crossley and Fowler, 1986) and increased (microscopic) leaf wettability (Burkhardt and Eiden, 1994; Burkhardt and Hunsche, 2013). It was suggested by many authors that polluted leaves retain water better. The formation of liquid water films and the enhanced scavenging of O₃ at wetted surfaces could be modulated by the presence of specific (deliquescent) particles deposited on the leaf cuticle, altering the cuticle uptake rates of the wetted leaves (Burkhardt and Eiden, 1994; Sun et al., 2016). It was evident from our analysis that occurrence of dewfall favored the O₃ deposition velocity, which was in agreement with other studies (Fuentes et al., 1992; Lamaud et al., 2002). It is generally postulated that wetting of the foliage by rain or dew leads to stomatal blocking during the summer daytime (Finkelstein et al., 2000). In case of a

dew-wetted canopy, it was observed that the skewed diurnal cycle of v_d in summer closely resembled that of a dry canopy, which follows the asymmetrical cycle of stomatal conductance (Fowler et al., 2009; Wu et al., 2016). This suggested that stomata weren't fully blocked and stomatal uptake could still proceed at a higher rate compared to a rain-wetted canopy. The high v_d recorded for a snow covered surface was in disagreement with the literature (Hardacre et al., 2015) but it must be emphasized that the snow cover on soil and canopy was very shallow and also included sleet.

Low levels of ground water table were also conducive to O₃ uptake. Mechanisms behind the chemical quenching at the soil surface are not completely understood but findings from several flux partitioning studies emphasized the soil as an important sink for O₃ in forests (Lamaud et al., 2002; Dorsey et al., 2004; Fares et al., 2014; Zhou et al., 2017) as well in ecosystems with smooth surfaces (Sanchez et al., 1997; Meszaros et al., 2009; Stella et al., 2013). The fact that low ground water levels favored O₃ uptake suggested that the depth or soil volume available for O₃ to diffuse in the soil pores constituted a limiting factor for uptake in the soil (Personne et al., 2015; Vuolo et al., 2017). A laboratory study, conducted by Sorimachi and Sakamoto (2007) on Chinese soil samples revealed that there was only a small impact of geometric surface area or soil weight on v_d . There was, however, a positive correlation with the relative humidity or the moisture content of the soil surface, which was in agreement with the literature (Hicks et al., 1987; Erisman et al., 1994; Stella et al., 2011). This was interpreted by the latter authors that wetter soils limited the rate of O₃ deposition in the soil because of decreased soil porosity and hence, reduced availability of reaction sites for O₃. Based on Massman (2004), Meszaros et al. (2009) used a relatively greater soil resistance for O₃ deposition for wet soils than for dry soils, although low soil moisture content could also induce soil moisture stress limiting stomatal uptake (Emberson et al., 2001). Low levels of ground water table, entail a low water filled porosity, which could additionally enhance biogenic NO emission on sandy textured soils, supporting coniferous forest (Pilegaard et al., 2006). Gas flux measurements from incubated soil and forest floor samples at our nitrogen-saturated site demonstrated the presence of NO-emission (Wagner, 2009). Emission of NO from the forest floor averaged $\pm 300 \mu\text{g N m}^{-2} \text{ h}^{-1}$. Highest rates of NO emission from the mineral top soil occurred at a water filled porosity of 50–60%.

A multivariate analysis was conducted to explain the annual deposition pattern of O₃ during the day and nighttime and to elucidate possible differences in v_d among the years over the period 2005–2015. Especially environmental variables, driving non-stomatal processes (chemical reactions, canopy wetness, soil uptake) contributed to explaining the annual pattern in v_d . Although the presence of NO_x led to enhanced daytime values of v_d during the entire winter period, there was a conspicuous tendency toward higher v_d s during autumn. The increased v_d s recorded during autumnal months at our site coincided with a seasonally dependent increased frequency of canopy wetness events, occurrence of needle senescence and the reaching of a minimum water table depth at the end of the growing season. Potier et al. (2015) concluded

that enhanced deposition of O_3 on wet senescing leaves of wheat was due to leaching of apoplastic antioxidants toward the leaf surface. Besides an altered chemical proclivity of wet senescent foliage for trapping O_3 , it is also conceivable that the decrease of LAI during the leaf-fall period, could allow for a better turbulent transfer of O_3 in the trunk space, enabling a better transport toward the forest soil. The overall effect of these mechanisms could be the reason for unexpected decreases in autumnal R_c , noticed at other forest sites (Klemm and Mangold, 2001).

The explained variability by the set of environmental variables was, however, rather low, even during the daytime (<30%). The model was not adequate enough to explain higher v_{ds} in substantially different weather conditions or explain the high inter-annual variability. This indicated that other unaccounted variables or drivers with a different meteorological signature, thwarted a thorough analysis of the controlling mechanisms behind the O_3 uptake at our site. During spring 2007, a serious drought impacted the forest, which entailed extremely low RH (high vapor pressure deficit and temperature). We surmise that these stress conditions, which were assumed to suppress O_3 uptake by limiting reactions onto wet surfaces or inducing stomatal closure, conversely triggered BVOC emissions, leading to O_3 quenching. Information about emission of storage or non-storage monoterpenes from the pine foliage, branches, stem or forest floor is, however, lacking at our site but BVOC measurements could have casted a light on the overly high O_3 fluxes, measured during spring 2007 or in other years with high O_3 dry deposition rates (e.g., 2010). Excessive springtime monoterpene emissions or standard emission rates were measured in *Pinus* stands as a consequence of drought stress (Bäck et al., 2005), springtime phase change in stem water transport capacity (Vanhatalo et al., 2015), bud break (Kim, 2001), general stress to the plant (Komenda and Koppmann, 2002) or disturbed tree-herbivore relations (Phillips and Croteau, 1999; Trowbridge et al., 2014). Emission of BVOCs from intact Scots pine branches can be very high in early spring, often much higher than the emission occurring later in the growing season (Tarvainen et al., 2005; Hakola et al., 2006). Especially solar radiation explained the largest part in the variability in F and v_d during the drought period (Figures 10, 11). The high reactivity of O_3 cannot solely be explained by stomatal uptake, because values of v_d were too high for the stomatal pathway ($>2\text{ cm s}^{-1}$). It is possible that light-dependent emissions of BVOCs mimicked the stomatal conductance dynamics, which are also driven by light and heat (Hogg et al., 2007). BVOCs released from the foliage could have dissolved in the epicuticular wax layers, where they play a role in chemical reactions with oxidizing agents as O_3 (Joensuu et al., 2016) or they take part in the formation of water layers, which enhance in turn the deposition of O_3 (Sumner et al., 2004). The strong dependence of v_d on light (solar radiation or photosynthetic photon flux density) can also be due to ozone photolysis (Rondon et al., 1993; Fowler et al., 2001; Hogg et al., 2007; Cape et al., 2009). Coyle et al. (2009) suggested that ozone could be removed at a (very) dry potato crop surface by thermal

decomposition, possibly enhanced by photo-chemical reactions in the daytime.

CONCLUSIONS

The study casts some light on the high deposition velocity of O_3 , measured at our suburban forest. There is evidence that the presence of a chemical sink during the working-weeks led to increased gas-phase reactions between O_3 and NO between the measuring height and the canopy surface. Average daytime fluxes were 13 and 6% higher during winter and summer working-weeks compared to the respective weekend values. NO emissions didn't solely originate from vehicle exhaust by diesel-powered engine cars in close proximity of the forest but also from the more remote intense traffic, chemical industries and petrochemical refineries, located at Antwerp port.

The O_3 deposition was further especially controlled by non-stomatal processes, such as deposition onto external wet surfaces. Especially a dew-wetted canopy was found to be a perfect O_3 sink. The study also showed that deposition was favored at the end of the growing season when ground water table reached its lowest level and in-canopy transfer was faster due to the drop in LAI. This lends support to the fact that soil uptake might also have been overlooked at our site for other pollutants (e.g., NH_3) and at other forest sites. Further flux partitioning research must scrutinize the transport of O_3 in the trunk space and the final deposition in the soil compartment. Direct flux measurements of O_3 to the forest floor would be very convenient to ascertain which soil conditions (water content, organic matter, amount of fresh litter . . .) enhance the removal at the soil surface.

The lacking information of monoterpenes at our site prevents a thorough analysis of the environmental control of O_3 removal at our site. The meteorological signature of BVOC triggers might be different than the ones controlling other non-stomatal or stomatal mechanisms behind O_3 removal. The convolution of those different effects in the total O_3 uptake renders a thorough analysis of controlling environmental variables increasingly intricate.

AUTHOR CONTRIBUTIONS

The corresponding author, JN is an atmospheric scientist and the manager of the research site. He validated the 10-year long dataset and performed the final analysis. He already published a paper about the ozone deposition at the site (Journal of Environmental Monitoring). He was assisted by his colleague AV, head of the ICP Forest Deposition panel. He is an R-wizzard and was helpful during the statistical analysis. He is also skilled in the deposition of nitrogen compounds, especially nitrogen oxides.

ACKNOWLEDGMENTS

This project was performed under the authority of the Flemish minister of Environment. We gratefully acknowledge Eddy Smesman (INBO) and the Flemish Environmental Agency (VMM) for the calibration and maintenance of the monitors.

REFERENCES

- Altimir, N., Kolari, P., Tuovinen, J. P., Vesala, T., Back, J., Suni, T., et al. (2006). Foliage surface ozone deposition: a role for surface moisture? *Biogeosciences* 3, 209–228. doi: 10.5194/bg-3-209-2006
- Ashmore, M. R. (2005). Assessing the future global impacts of ozone on vegetation. *Plant Cell Environ.* 28, 949–964. doi: 10.1111/j.1365-3040.2005.01341.x
- Bäck, J., Hari, P., Hakola, H., Juurola, E., and Kulmala, M. (2005). Dynamics of monoterpene emissions in *Pinus sylvestris* during early spring. *Boreal Env. Res.* 10, 409–424.
- Beljaars, A. C. L., and Holtstag, A. A. M. (1990). Description of a software library for the calculation of surface fluxes *Environ. Softw.* 5, 60–68. doi: 10.1016/0266-9838(90)90002-N
- Bosveld, F. C. (1991). *Exchange Coefficients over a Douglas Fir Forest Dutch Priority Programme on Acidification, Project 1901 Royal Netherlands Meteorological Institute (KNMI)* (De Bilt).
- Burkhardt, J., and Eiden, R. (1994). Thin water films on coniferous needles. *Atmos. Environ.* 28, 2001–2017. doi: 10.1016/1352-2310(94)90469-3
- Burkhardt, J., and Hunsche, M. (2013). “Breath figures” on leaf surface-formation and effects of microscopic leaf wetness. *Front. Plant Sci.* 4:422. doi: 10.3389/fpls.2013.00422
- Businger, J. A., Wyngaard, J. C., Izumi, Y., and Bradley, E. F. (1970). Flux-profile relationships in the atmospheric surface layer. *J. Atmos. Sci.* 28, 181–189. doi: 10.1175/1520-0469(1971)028<0181:FPRITA>2.0.CO;2
- Cape, J. N., Hamilton, R., and Heal, M. R. (2009). Reactive uptake of ozone at simulated leaf surfaces: implications for ‘non-stomatal’ ozone flux. *Atmos. Environ.* 43, 1116–1123. doi: 10.1016/j.atmosenv.2008.11.007
- Carrara, A., Kowalski, A. S., Neiryck, J., Janssens, I. A., Yuste, J. C., and Ceulemans, R. (2003). Net ecosystem CO₂ exchange of mixed forest in Belgium over 5 years. *Agric. For. Meteorol.* 119, 209–227. doi: 10.1016/S0168-1923(03)00120-5
- Clifton, O. E., Fiore, A. M., Munger, J. W., Malyshev, S., Horowitz, L. W., Shevliakova, E., et al. (2017). Interannual variability in ozone removal by a temperate deciduous forest. *Geophys. Res. Lett.* 44, 542–552. doi: 10.1002/2016GL070923
- Coyle, M., Nemitz, E., Storeton-West, R., Fowler, D., and Cape, J. N. (2009). Measurements of ozone deposition to a potato canopy. *Agric. For. Meteorol.* 149, 655–666. doi: 10.1016/j.agrformet.2008.10.020
- Crossley, A., and Fowler, D. (1986). The weathering of scots pine epicuticular wax in polluted and clean-air. *N. Phytol.* 103, 207–218. doi: 10.1111/j.1469-8137.1986.tb00609.x
- Damköhler, G. (1940). Der Einfluss der Turbulenz auf die Flammgeschwindigkeit in Gasgemischen. *Z. Elektrochem. Angew.* 46, 601–652. doi: 10.1002/bbpc.19400461102
- de Vries, W., Dobbertin, M. H., Solberg, S., van Dobben, H. F., and Schaub, M. (2014). Impacts of acid deposition, ozone exposure and weather conditions on forest ecosystems in Europe: an overview. *Plant Soil* 380, 1–45. doi: 10.1007/s11104-014-2056-2
- Dorsey, J. R., Duyzer, J. H., Gallagher, M. W., Coe, H., Pilegaard, K., Weststrate, J. H., et al. (2004). Oxidized nitrogen and ozone interaction with forests. I: experimental observations and analysis of exchange with douglas fir. *Q. J. R. Meteorol. Soc.* 130, 1941–1955. doi: 10.1256/qj.03.124
- Dyer, A. J., and Hicks, B. B. (1970). Flux-gradient relationships in the constant flux layer. *Q. J. R. Meteorol. Soc.* 96, 715–721. doi: 10.1002/qj.49709641012
- Emberson, L. D., Ashmore, M. R., Simpson, D., Tuovinen, J. P., and Cambridge, H. M. (2001). Modelling and mapping ozone deposition in Europe. *Water Air Soil Pollut.* 130, 577–582. doi: 10.1023/A:1013851116524
- Erisman, J. W., Vanpul, A., and Wyers, P. (1994). Parametrization of surface-resistance for the quantification of atmospheric deposition of acidifying pollutants and ozone. *Atmos. Environ.* 28, 2595–2607. doi: 10.1016/1352-2310(94)90433-2
- Fares, S., McKay, M., Holzinger, R., and Goldstein, A. H. (2010). Ozone fluxes in a *Pinus ponderosa* ecosystem are dominated by non-stomatal processes: evidence from long-term continuous measurements. *Agric. For. Meteorol.* 150, 420–431. doi: 10.1016/j.agrformet.2010.01.007
- Fares, S., Savi, F., Muller, J., Matteucci, G., and Paoletti, E. (2014). Simultaneous measurements of above and below canopy ozone fluxes help partitioning ozone deposition between its various sinks in a Mediterranean Oak forest. *Agric. For. Meteorol.* 198, 181–191. doi: 10.1016/j.agrformet.2014.08.014
- Finkelstein, P. L., Ellestad, T. G., Clarke, J. F., Meyers, T. P., Schwede, D. B., Hebert, E. O., et al. (2000). Ozone and sulfur dioxide dry deposition to forests: observations and model evaluation. *J. Geophys. Res.-Atmos.* 105, 15365–15377. doi: 10.1029/2000JD900185
- Fowler, D., Cape, J. N., Coyle, M., Flechard, C., Kuylenstierna, J., Hicks, K., et al. (1999). The global exposure of forests to air pollutants. *Water Air Soil Pollut.* 116, 5–32. doi: 10.1023/A:1005249231882
- Fowler, D., Flechard, C., Cape, J. N., Storeton-West, R. L., and Coyle, M. (2001). Measurements of ozone deposition to vegetation quantifying the flux, the stomatal and non-stomatal components. *Water Air Soil Pollut.* 130, 63–74. doi: 10.1023/A:1012243317471
- Fowler, D., Pilegaard, K., Sutton, M. A., Ambus, P., Raivonen, M., Duyzer, J., et al. (2009). Atmospheric composition change: ecosystems-atmosphere interactions. *Atmos. Environ.* 43, 5193–5267. doi: 10.1016/j.atmosenv.2009.07.068
- Franz, M., Simpson, D., Arneth, A., and Zaehle, S. (2017). Development and evaluation of an ozone deposition scheme for coupling to a terrestrial biosphere model. *Biogeosciences* 14, 45–71. doi: 10.5194/bg-14-45-2017
- Fuentes, J. D., Gillespie, T. J., Denhartog, G., and Neumann, H. H. (1992). Ozone deposition onto a deciduous forest during dry and wet conditions. *Agric. For. Meteorol.* 62, 1–18. doi: 10.1016/0168-1923(92)90002-L
- Fuhrer, J., Val Martin, M. V., Mills, G., Heald, C. L., Harmens, H., Hayes, F., et al. (2016). Current and future ozone risks to global terrestrial biodiversity and ecosystem processes. *Ecol. Evol.* 6, 8785–8799. doi: 10.1002/ece3.2568
- Fujita, E. M., Stockwell, W. R., Campbell, D. E., Keislar, R. E., and Lawson, D. R. (2003). Evolution of the magnitude and spatial extent of the weekend ozone effect in California’s South Coast Air Basin, 1981–2000. *J. Air Waste Manage. Assoc.* 53, 802–815. doi: 10.1080/10473289.2003.10466225
- Garland, J. A. (1978). Dry and wet removal of sulfur from atmosphere. *Atmos. Environ.* 12, 349–362. doi: 10.1016/0004-6981(78)90217-2
- Hakola, H., Tarvainen, V., Back, J., Ranta, H., Bonn, B., Rinne, J., et al. (2006). Seasonal variation of mono- and sesquiterpene emission rates of Scots pine. *Biogeosciences* 3, 93–101. doi: 10.5194/bg-3-93-2006
- Hardacre, C., Wild, O., and Emberson, L. (2015). An evaluation of ozone dry deposition in global scale chemistry climate models. *Atmos. Chem. Phys.* 15, 6419–6436. doi: 10.5194/acp-15-6419-2015
- Hicks, B. B., Baldocchi, D. D., Meyers, T. P., Hosker, R. P., and Matt, D. R. (1987). A preliminary multiple resistance routine for deriving dry deposition velocities from measured quantities. *Water Air Soil Pollut.* 36, 311–330. doi: 10.1007/BF00229675
- Hogg, A., Uddling, J., Ellsworth, D., Carroll, M. A., Pressley, S., Lamb, B., et al. (2007). Stomatal and non-stomatal fluxes of ozone to a northern mixed hardwood forest. *Tellus Ser. B Chem. Phys. Meteorol.* 59, 514–525. doi: 10.1111/j.1600-0889.2007.00269.x
- Hoshika, Y., Katata, G., Deushi, M., Watanabe, M., Koike, T., and Paoletti, E. (2015). Ozone-induced stomatal sluggishness changes carbon and water balance of temperate deciduous forests. *Sci. Rep.* 5:9871. doi: 10.1038/srep09871
- IPCC (2007). *Climate Change 2007: Synthesis Report. Contribution of Working Groups I, II and III to the Fourth Assessment Report of the Intergovernmental Panel on Climate Change*, eds Core Writing Team, R. K. Pachauri, and A. Reisinger (Geneva: IPCC).
- Joensuu, J., Altimir, N., Hakola, H., Rostas, M., Raivonen, M., Vestenius, M., et al. (2016). Role of needle surface waxes in dynamic exchange of mono- and sesquiterpenes. *Atmos. Chem. Phys.* 16, 7813–7823. doi: 10.5194/acp-16-7813-2016
- Kim, J. C. (2001). Factors controlling natural VOC emissions in a southeastern US pine forest. *Atmos. Environ.* 35, 3279–3292. doi: 10.1016/S1352-2310(00)00522-7

- Klemm, O., and Mangold, A. (2001). Ozone deposition at a forest site in NE Bavaria. *Water Air Soil Pollut.: Focus* 1, 223–232. doi: 10.1023/A:1013167408114
- Klingberg, J., Engardt, M., Karlsson, P. E., Langner, J., and Pleijel, H. (2014). Declining ozone exposure of European vegetation under climate change and reduced precursor emissions. *Biogeosciences* 11, 5269–5283. doi: 10.5194/bg-11-5269-2014
- Komenda, M., and Koppmann, R. (2002). Monoterpene emissions from scots pine (*Pinus sylvestris*): field studies of emission rate variabilities. *J. Geophys. Res. Atmos.* 107, ACH 1-1–ACH 1-13. doi: 10.1029/2001JD000691
- Lamaud, E., Carrara, A., Brunet, Y., Lopez, A., and Druilhet, A. (2002). Ozone fluxes above and within a pine forest canopy in dry and wet conditions. *Atmos. Environ.* 36, 77–88. doi: 10.1016/S1352-2310(01)00468-X
- Lenschow, D. H. (1982). Reactive trace species in the boundary-layer from a micrometeorological perspective. *J. Meteorol. Soc. Japan* 60, 472–480. doi: 10.2151/jmsj1965.60.1_472
- Massman, W. J. (2004). Toward an ozone standard to protect vegetation based on effective dose: a review of deposition resistances and a possible metric. *Atmos. Environ.* 38, 2323–2337. doi: 10.1016/j.atmosenv.2003.09.079
- Meszaros, R., Horvath, L., Weidinger, T., Neftel, A., Nemitz, E., Dammgen, U., et al. (2009). Measurement and modelling ozone fluxes over a cut and fertilized grassland. *Biogeosciences* 6, 1987–1999. doi: 10.5194/bg-6-1987-2009
- Mikkelsen, T. N., Ro-Poulsen, H., Hovmand, M. F., Jensen, N. O., Pilegaard, K., and Egelov, A. H. (2004). Five-year measurements of ozone fluxes to a Danish Norway spruce canopy. *Atmos. Environ.* 38, 2361–2371. doi: 10.1016/j.atmosenv.2003.12.036
- Mills, G., Harmens, H., Wagg, S., Sharps, K., Hayes, F., Fowler, D., et al. (2016). Ozone impacts on vegetation in a nitrogen enriched and changing climate. *Environ. Pollut.* 208, 898–908. doi: 10.1016/j.envpol.2015.09.038
- Monteith, J. L. and Unsworth, M. H. (1990). *Principles of Environmental Physics*. 2nd edn. London: Edward Arnold.
- Monin, A. S., Obukhov, A. M. (1954). Basic laws of turbulence mixing in the ground layer of the atmosphere. *Acad. NaukSSRTrudGeofizInst.* 24, 163–187.
- Neiryck, J., Flechard, C. R., and Fowler, D. (2011). Long-term (13 years) measurements of SO₂ fluxes over a forest and their control by surface chemistry. *Agric. For. Meteorol.* 151, 1768–1780. doi: 10.1016/j.agrformet.2011.07.013
- Neiryck, J., Gielen, B., Janssens, I. A., and Ceulemans, R. (2012). Insights into ozone deposition patterns from decade-long ozone flux measurements over a mixed temperate forest. *J. Environ. Monit.* 14, 1684–1695. doi: 10.1039/c2em10937a
- Neiryck, J., Kowalski, A. S., Carrara, A., and Ceulemans, R. (2005). Driving forces for ammonia fluxes over mixed forest subjected to high deposition loads. *Atmos. Environ.* 39, 5013–5024. doi: 10.1016/j.atmosenv.2005.05.027
- Neiryck, J., Kowalski, A. S., Carrara, A., Genouw, G., Berghmans, P., and Ceulemans, R. (2007). Fluxes of oxidised and reduced nitrogen above a mixed coniferous forest exposed to various nitrogen emission sources. *Environ. Pollut.* 149, 31–43. doi: 10.1016/j.envpol.2006.12.029
- Paoletti, E., and Grulke, N. E. (2010). Ozone exposure and stomatal sluggishness in different plant physiognomic classes. *Environ. Pollut.* 158, 2664–2671. doi: 10.1016/j.envpol.2010.04.024
- Personne, E., Tardy, F., Genermont, S., Decuq, C., Gueudet, J. C., Mascher, N., et al. (2015). Investigating sources and sinks for ammonia exchanges between the atmosphere and a wheat canopy following slurry application with trailing hose. *Agric. For. Meteorol.* 207, 11–23. doi: 10.1016/j.agrformet.2015.03.002
- Phillips, M. A., and Croteau, R. B. (1999). Resin-based defenses in conifers. *Trends Plant Sci.* 4, 184–190. doi: 10.1016/S1360-1385(99)01401-6
- Pilegaard, K., Skiba, U., Ambus, P., Beier, C., Brüggemann, N., Butterbach-Bahl, K., et al. (2006). Factors controlling regional differences in forest soil emission of nitrogen oxides (NO and N₂O). *Biogeosciences* 3, 651–661. doi: 10.5194/bg-3-651-2006
- Potier, E., Ogee, J., Jouanguy, J., Lamaud, E., Stella, P., Personne, E., et al. (2015). Multi layer modelling of ozone fluxes on winter wheat reveals large deposition on wet senescing leaves. *Agricul. For. Meteorol.* 211, 58–71. doi: 10.1016/j.agrformet.2015.05.006
- Rannik, U., Altimir, N., Mammarella, I., Back, J., Rinne, J., Ruuskanen, T. M., et al. (2012). Ozone deposition into a boreal forest over a decade of observations: evaluating deposition partitioning and driving variables. *Atmos. Chem. Phys.* 12, 12165–12182. doi: 10.5194/acp-12-12165-2012
- R Development Core Team (2015). *A Language and Environment for Statistical Computing*. Vienna: R Foundation for Statistical Computing. Available online at: www.R-project.org/ (Accessed July 23, 2015).
- Rondon, A., Johansson, C., and Granat, L. (1993). Dry deposition of nitrogen-dioxide and ozone to coniferous forests. *J. Geophys. Res. Atmos.* 98, 5159–5172. doi: 10.1029/92J.D.02335
- Sanchez, M. L., Rodriguez, R., and Lopez, A. (1997). Ozone dry deposition in a semi-arid steppe and in a coniferous forest in southern Europe. *J. Air Waste Manage. Assoc.* 47, 792–799. doi: 10.1080/10473289.1997.10463939
- Schreuder, M. D. J., van Hove, L. W. A., and Brewer, C. A. (2001). Ozone exposure affects leaf wettability and tree water balance. *N. Phytologist* 152, 443–454. doi: 10.1046/j.0028-646X.2001.00272.x
- Sicard, P., Anav, A., De Marco, A., and Paoletti, E. (2017). Projected global ground-level ozone impacts on vegetation under different emission and climate scenarios. *Atmos. Chem. Phys.* 17, 12177–12196. doi: 10.5194/acp-17-12177-2017
- Sorimachi, A., and Sakamoto, K. (2007). Laboratory measurement of dry deposition of ozone onto northern chinese soil samples. *Water Air Soil Pollut. Focus* 7, 181–186. doi: 10.1007/s11267-006-9098-2
- Stella, P., Loubet, B., Lamaud, E., Laville, P., and Cellier, P. (2011). Ozone deposition onto bare soil: a new parameterisation. *Agric. For. Meteorol.* 151, 669–681. doi: 10.1016/j.agrformet.2011.01.015
- Stella, P., Loubet, B., Laville, P., Lamaud, E., Cazaunau, M., Laufs, S., et al. (2012). Comparison of methods for the determination of NO-O₃-NO₂ fluxes and chemical interactions over a bare soil. *Atmos. Meas. Tech.* 5, 1241–1257. doi: 10.5194/amt-5-1241-2012
- Stella, P., Personne, E., Lamaud, E., Loubet, B., Trebs, I., and Cellier, P. (2013). Assessment of the total, stomatal, cuticular, and soil 2 year ozone budgets of an agricultural field with winter wheat and maize crops. *J. Geophys. Res. Biogeosci.* 118, 1120–1132. doi: 10.1002/jgrg.20094
- Sumner, A. L., Menke, E. J., Dubowski, Y., Newberg, J. T., Penner, R. M., Hemminger, J. C., et al. (2004). The nature of water on surfaces of laboratory systems and implications for heterogeneous chemistry in the troposphere. *Phys. Chem. Chem. Phys.* 6, 604–613. doi: 10.1039/b308125g
- Sun, S., Moravek, A., Trebs, I., Kesselmeier, J., and Sorgel, M. (2016). Investigation of the influence of liquid surface films on O₃ and PAN deposition to plant leaves coated with organic/inorganic solution. *J. Geophys. Res.-Atmos.* 121, 14239–14256. doi: 10.1002/2016JD025519
- Tarvainen, V., Hakola, H., Hellen, H., Back, J., Hari, P., and Kulmala, M. (2005). Temperature and light dependence of the VOC emissions of Scots pine. *Atmos. Chem. Phys.* 5, 989–998. doi: 10.5194/acp-5-989-2005
- Trowbridge, A. M., Daly, R. W., Helmig, D., Stoy, P. C., and Monson, R. K. (2014). Herbivory and climate interact serially to control monoterpene emissions from pinyon pine forests. *Ecology* 95, 1591–1603. doi: 10.1890/13-0989.1
- Vanhatalo, A., Chan, T., Aalto, J., Korhonen, J. F., Kolari, P., Holttä, T., et al. (2015). Tree water relations can trigger monoterpene emissions from Scots pine stems during spring recovery. *Biogeosciences* 12, 5353–5363. doi: 10.5194/bg-12-5353-2015
- Vilà-Guerau de Arellano, J., and Duykerke, P. G. (1992). Influence of chemistry on the flux-gradient relationships for the NO-O₃-NO₂ system. *Boundary-Layer Meteorol.* 61, 375–387. doi: 10.1007/BF00119098
- Vuolo, R. M., Loubet, B., Mascher, N., Gueudet, J. C., Durand, B., Laville, P., et al. (2017). Nitrogen oxides and ozone fluxes from an oilseed-rape management cycle: the influence of cattle slurry application. *Biogeosciences* 14, 2225–2244. doi: 10.5194/bg-14-2225-2017
- Wagner, D. (2009). *Climate change effects on greenhouse gas emissions from Northern European Soils*. Vienna: Diplomstudium Theoret./Angewandte Geographie, University of Wien.
- World Health Organization (WHO) (2008). *The World Health Report 2008: Primary Health Care – Now More Than Ever* (Geneva).
- Wolff, G. T., Kahlbaum, D. F., and Heuss, J. M. (2013). The vanishing ozone weekday/weekend effect. *J. Air Waste Manage. Assoc.* 63, 292–299. doi: 10.1080/10962247.2012.749312

- Wu, Z. Y., Staebler, R., Vet, R., and Zhang, L. M. (2016). Dry deposition of O₃ and SO₂ estimated from gradient measurements above a temperate mixed forest. *Environ. Pollut.* 210, 202–210. doi: 10.1016/j.envpol.2015.11.052
- Zhang, L., Wang, T., Zhang, Q., Zheng, J. Y., Xu, Z., and Lv, M. Y. (2016). Potential sources of nitrous acid (HONO) and their impacts on ozone: a WRF-chem study in a polluted subtropical region. *J. Geophys. Res. Atmos.* 121, 3645–3662. doi: 10.1002/2015JD024468
- Zhou, P. T., Ganzeveld, L., Rannik, U., Zhou, L. X., Gierens, R., Taipale, D., et al. (2017). Simulating ozone dry deposition at a boreal forest with a multi-layer canopy deposition model. *Atmos. Chem. Phys.* 17, 1361–1379. doi: 10.5194/acp-17-1361-2017

Conflict of Interest Statement: The authors declare that the research was conducted in the absence of any commercial or financial relationships that could be construed as a potential conflict of interest.

Copyright © 2018 Neiryck and Verstraeten. This is an open-access article distributed under the terms of the Creative Commons Attribution License (CC BY). The use, distribution or reproduction in other forums is permitted, provided the original author(s) and the copyright owner(s) are credited and that the original publication in this journal is cited, in accordance with accepted academic practice. No use, distribution or reproduction is permitted which does not comply with these terms.